Quenching and amplification of thermoacoustic oscillations in two nonidentical Rijke tubes interacting via time-delay and dissipative coupling

Mohammad Hossein Doranehgard[*]

Department of Mechanical and Aerospace Engineering, The Hong Kong University of Science and Technology, Clear Water Bay, Hong Kong

Vikrant Gupta

Department of Mechanics and Aerospace Engineering, Southern University of Science and Technology, Shenzhen, China
and Guangdong–Hong-Kong–Macao Joint Laboratory for Data-Driven Fluid Mechanics and Engineering Applications,
Southern University of Science and Technology, Shenzhen, China

Larry K. B. Li [†]

Department of Mechanical and Aerospace Engineering, The Hong Kong University of Science and Technology, Clear Water Bay, Hong Kong
and Guangdong–Hong-Kong–Macao Joint Laboratory for Data-Driven Fluid Mechanics and Engineering Applications,
The Hong Kong University of Science and Technology, Clear Water Bay, Hong Kong

We numerically explore the quenching and amplification of self-excited thermoacoustic oscillations in two nonidentical Rijke tubes interacting via time-delay and dissipative coupling. On applying either type of coupling separately, we find that the presence of nonidentical heater powers can shrink the regions of amplitude death in both oscillators, while producing new regions of amplitude amplification in the weaker oscillator. We find that the magnitude of amplitude amplification grows with the heater power mismatch and with the total power input. These effects are also present when both types of coupling are applied simultaneously. This study highlights the critical role that nonidentical thermal loads can play in determining the amplitude response of coupled thermoacoustic systems, facilitating the design of control strategies for coupled oscillatorlike devices such as gas turbines.

I. INTRODUCTION

When two or more self-excited oscillators interact via coupling, they can develop a variety of collective multiscale behaviors, as manifested through adjustments in their phase and amplitude dynamics [1]. If the coupling is weak, mutual synchronization can occur, leading to frequency or phase locking between identical or nonidentical oscillators [2,3]. By contrast, if the coupling is strong, oscillation quenching can occur, leading to amplitude death–a state in which all the oscillators of the system stop, with their phase trajectories converging to the same stable fixed point [4–6].

The collective behavior of a coupled oscillator system depends not only on the coupling strength, but also on the coupling type. Previous studies have shown that amplitude death can be induced by various types of coupling, such as dissipative coupling, time-delay coupling, conjugate coupling, and nonlinear coupling [7]. Unsurprisingly, this has led to amplitude death being detected in various systems, such as electronic circuits [8], thermokinetic systems [9], and chemical reactions [10].

Besides the coupling parameters, the individual oscillator parameters may also influence the emergent behavior [3], but their effect remains a topic of active research,

particularly in the field of thermoacoustics [11]. In thermoacoustic systems, heat-release-rate (HRR) and pressure fluctuations can interact in positive feedback to generate self-excited flow oscillations via the Rayleigh mechanism [4]. At high amplitudes, such thermoacoustic oscillations can exacerbate thermal and mechanical stresses [12], and induce flame blowout and flashback [13], reducing the efficiency, operability, and reliability of devices such as gas turbines, domestic boilers, and rocket engines [14,15]. It is therefore important to determine the system and coupling parameters for which thermoacoustic oscillations become quenched or amplified [16–19].

Previous work on passive and active control of thermoacoustic oscillations has focused mostly on systems with isolated acoustic chambers (e.g., single combustors) [14,16,20–27]. This is because such systems exhibit relatively simple geometries and well-defined boundary conditions, facilitating simulation, experimentation, and analysis [28]. By contrast, the thermoacoustics of coupled oscillator systems has been studied less extensively, despite their relevance to practical devices such as can-annular gas turbines [29–33]. Crucially, it is widely acknowledged that the collective behavior of a coupled thermoacoustic system cannot simply be inferred from the individual behavior of its constitute oscillators in isolation [18,19]. This is because acoustic interactions can occur between oscillators, producing complex collective dynamics that can be difficult to predict within a single oscillator framework based on reductionism [11,34].

[*]mhd@connect.ust.hk

[†]larryli@ust.hk

By adopting a coupled oscillator framework, several researchers have been able to identify states of oscillation quenching suitable for suppressing thermoacoustic instability [18,19,35]. Prime among these is amplitude death, which, as noted earlier, occurs when all the oscillators of a coupled system become quenched to a common steady state [5]. Amplitude death has proved to be an effective mechanism for disrupting the feedback loop between sound waves and unsteady heat release. Thermoacoustic experiments within the past decade have shown that amplitude death can be found in both laminar systems (e.g., those powered by Bunsen flames [36], electrically heated meshes [37], and porous stacks [38,39]) and turbulent systems (e.g., those powered by lean-premixed flames [35,40,41]). Besides amplitude death, other nonlinear phenomena have also been reported, such as partial amplitude death, in-phase and antiphase synchronization, and phase-flip bifurcations [37]; the latter refer to an abrupt transition between in-phase and antiphase synchronization when a coupling parameter is varied [42]. Despite various contributions from experiments, remarkable insight can still be gained by analyzing low-order models of coupled oscillator systems. For example, modeling studies have shown that achieving amplitude death in a purely dissipatively coupled system requires the natural frequencies of the oscillators to be sufficiently different, i.e., the detuning must be sufficiently large [43,44]. However, achieving amplitude death in a purely time-delay coupled system requires no detuning, provided that the coupling strength and delay time are appropriate [44,45]. Importantly, if dissipative and time-delay coupling are applied simultaneously, then the parameter region corresponding to amplitude death grows in size [38,44].

The above review would suggest that a potential way to suppress thermoacoustic oscillations might be to induce amplitude death by carefully adjusting the system parameters (e.g., detuning) and the coupling parameters (e.g., type and strength). However, most previous studies on coupled thermoacoustic systems have focused on the idealized case of identical oscillators, i.e., oscillators with identical limit-cycle frequencies and amplitudes before coupling is applied. Although some studies—most notably that by Thomas *et al.* [44]—have considered the effect of nonidentical oscillators, the full extent of the parameter space has yet to be systematically explored. This is important because, in practical devices, even oscillators built with identical dimensions and identical materials will rarely exhibit identical limit-cycle oscillations. Besides amplitude death, another situation worth examining is when the limit-cycle amplitude of an uncoupled oscillator becomes amplified due to coupling—a state we refer to here as *amplitude amplification*. This state is just as important as amplitude death itself because in some devices (e.g., pulse combustors [46] and solid-state lasers [47]), it is not sufficient to just avoid amplitude death, but also necessary to maintain or even amplify the self-excited oscillations. Thus, it is important to understand how the presence of mismatches in the initial (uncoupled) limit-cycle features of a coupled oscillator system can influence its quenching and amplification behavior.

In this numerical study, we explore the effect of nonidentical heater powers on the quenching and amplification of

two self-excited thermoacoustic oscillators, each modeled as a prototypical Rijke tube. We couple the two oscillators together via dissipative coupling only, then via time-delay coupling only, and finally via both dissipative and time-delay coupling. We show that irrespective of the coupling type, increasing the heater power mismatch can shrink the regions of amplitude death in both oscillators, while creating new regions of amplitude amplification in the weaker oscillator. This study highlights the important role that nonidentical thermal loads can play in determining the parameter space over which amplitude death and amplitude amplification occur in coupled thermoacoustic systems.

This paper is organized as follows. We present the low-order modeling framework in Sec. II and discuss the results in Sec. III, beginning with the dissipatively coupled system (Sec. III A), then the time-delay coupled system (Sec. III B), and finally the dissipatively and time-delay coupled system (Sec. III C). In Sec. IV, we conclude with the key findings of this study and general implications for the design of coupled oscillator systems.

II. LOW-ORDER THERMOACOUSTIC MODEL

We consider a prototypical thermoacoustic system consisting of two Rijke tube oscillators interacting via time-delay and dissipative coupling. Each Rijke tube oscillator is modeled as a horizontal acoustic duct containing a compact cylindrical heater [44,48]. This thermoacoustic model is chosen for two reasons [49]: (i) its low dimensionality and well-defined boundary conditions mean that its solutions can be computed readily with standard numerical schemes, and (ii) it contains the essential flow physics required to capture the complex nonlinear dynamics of coupled thermoacoustic systems. For these reasons, several previous studies have also adopted a similar Rijke tube model [44,48,50].

Following Balasubramanian and Sujith [48], and Thomas *et al.* [44], we start with the linearized forms of the momentum and energy equations for an acoustic field with a negligible mean temperature gradient,

$$\overline{\rho}^* \frac{\partial u'^*}{\partial t^*} + \frac{\partial p'^*}{\partial x^*} = 0, \tag{1}$$

$$\frac{\partial p'^*}{\partial t^*} + \gamma \overline{p}^* \frac{\partial u'^*}{\partial x^*} = (\gamma - 1)\dot{Q}'^* \delta(x^* - x_h^*), \tag{2}$$

where the superscript $*$ denotes dimensional quantities. Here, t^*, x^*, and x_h^* denote time, the position along the duct, and the position of the heater, respectively. Moreover, p'^*, u'^*, γ, and $\overline{\rho}^*$ denote the acoustic pressure, the acoustic velocity, the specific-heat ratio, and the mean fluid density, respectively. The heater is modeled as a set of wires producing HRR fluctuations per unit area $\dot{Q}'^*$ that are localized in space by the Dirac delta function δ. The heater is positioned at $x_h^* = l^*/4$ ($l^* \equiv$ the duct length), which is ideal for producing self-excited thermoacoustic oscillations in a Rijke tube.

The acoustic duct is open at both ends, implying that $p'^* = 0$ at the system boundaries ($x^* = 0$ and l^*), with the instantaneous pressure p^* there being equal to the time-averaged

pressure $\overline{p}^*$. To parametrize the governing equations [Eqs. (1) and (2)], we define the following dimensionless variables (without the superscript $*$):

$$x \equiv \frac{x^*}{l^*}, \quad t \equiv \frac{t^*}{l^*/c_0^*}, \quad u' \equiv \frac{u'^*}{u_0^*},$$

$$p' \equiv \frac{p'^*}{\overline{p}^*}, \quad \dot{Q}' \equiv \frac{\dot{Q}'^*}{\overline{p}^* c_0^*}, \quad M \equiv \frac{u_0^*}{c_0^*}, \quad (3)$$

where M, u_0, and c_0 denote the mean-flow Mach number, the steady-state velocity, and the speed of sound, respectively. Substituting the variables from Eq. (3) into Eqs. (1) and (2), we obtain the following dimensionless momentum and energy equations:

$$\gamma M \frac{\partial u'}{\partial t} + \frac{\partial p'}{\partial t} = 0, \quad (4)$$

$$\frac{\partial p'}{\partial t} + \gamma M \frac{\partial u'}{\partial x} + \zeta p' = (\gamma - 1)\dot{Q}'\delta(x - x_h), \quad (5)$$

where ζ is a damping coefficient whose value will be set later. We use a modified version of King's law to model the quasisteady heat transfer from the heater to the surrounding fluid [51,52],

$$\dot{Q}'(t) = \frac{2L_h(T_h - \overline{T})}{S\sqrt{3}c_0\overline{p}}\sqrt{\pi\lambda C_v u_0\overline{\rho}R_h}$$

$$\times \left[\sqrt{\left|\frac{1}{3} + u_h'(t - \tau_h)\right|} - \sqrt{\frac{1}{3}}\right], \quad (6)$$

where T_h, R_h, and L_h denote the temperature, radius, and length of the heater, respectively. Furthermore, C_v, λ, and $\overline{T}$ denote, respectively, the constant-volume specific heat, the thermal conductivity, and the mean fluid temperature in the acoustic duct of cross-sectional area S. When an acoustic perturbation arrives at the heater, a finite time passes before a resultant heat-transfer perturbation occurs. Following Subramanian *et al.* [50] and Heckl [52], we model this thermal-inertial effect with the time lag parameter τ_h acting on the acoustic velocity at the heater, $u_h'(t - \tau_h)$.

By inserting the HRR model [Eq. (6)] into the energy equation [Eq. (5)], we get [44,50]

$$\frac{\partial p'}{\partial t} + \gamma M \frac{\partial u'}{\partial x} + \zeta p'$$

$$= (\gamma - 1)\frac{2L_h(T_h - \overline{T})}{S\sqrt{3}c_0\overline{p}}\sqrt{\pi\lambda C_v u_0\overline{\rho}R_h}$$

$$\times \left[\sqrt{\left|\frac{1}{3} + u_h'(t - \tau_h)\right|} - \sqrt{\frac{1}{3}}\right]\delta(x - x_h). \quad (7)$$

Next we use the Galerkin technique to simplify the system of partial differential equations [PDEs, Eqs. (4) and (7)] into a system of ordinary differential equations (ODEs). To do this, we expand the acoustic velocity and pressure in terms of basis functions (Galerkin modes)

representing the natural acoustic duct modes with no heat input [44,50],

$$u' = \sum_{j=1}^{N} \eta_j \cos(j\pi x), \quad (8)$$

$$p' = -\sum_{j=1}^{N} \dot{\eta}_j \frac{\gamma M}{j\pi} \sin(j\pi x), \quad (9)$$

where η_j and $\dot{\eta}_j$ denote, respectively, the time-varying expansion coefficients for the acoustic velocity (u') and the acoustic pressure (p'). Together, Eqs. (8) and (9) constitute a complete basis, subject to the boundary condition $p' = 0$ at both ends of the duct. In our analysis, we use the first 10 Galerkin modes ($N = 10$) because it has been shown previously that the solution does not improve significantly with the inclusion of further modes [50].

By substituting the Galerkin expansion [Eqs. (8) and (9)] into the PDE system [Eqs. (4) and (7)], we obtain the following ODE system [44,48]:

$$\frac{d\eta_j}{dt} = \dot{\eta}_j, \quad (10)$$

$$\frac{d\dot{\eta}_j}{dt} + 2\zeta_j\omega_j\dot{\eta}_j + \omega_j^2\eta_j$$

$$= -j\pi K\left[\sqrt{\left|\frac{1}{3} + u_h'(t - \tau_h)\right|} - \sqrt{\frac{1}{3}}\right]\sin(j\pi x_h), \quad (11)$$

where the jth duct mode (Galerkin mode) has angular frequency $\omega_j = j\pi$. We account for frequency-dependent dissipation via the damping coefficient [53,54],

$$\zeta_j = \frac{1}{2\pi}\left[c_1\frac{\omega_j}{\omega_1} + c_2\sqrt{\frac{\omega_1}{\omega_j}}\right], \quad (12)$$

where the parameter values ($c_1 = 0.1$, $c_2 = 0.06$) are chosen based on the analysis by Thomas *et al.* [44]. The dimensionless heater power is defined as

$$K \equiv 4(\gamma - 1)\frac{L_h(T_h - \overline{T})}{M\gamma S\sqrt{3}c_0\overline{p}}\sqrt{\pi\lambda C_v u_0\overline{\rho}R_h}, \quad (13)$$

where all the parameter values are chosen based on the analysis by Balasubramanian and Sujith [48].

To establish a reference condition, we first consider a single (uncoupled) Rijke tube oscillator. We examine its temporal evolution by numerically solving the ODE system described above [Eqs. (10) to (13)]. Figure 1 shows the bifurcation diagram, with K as the bifurcation parameter. Along the forward path (increasing K), the root-mean-square pressure fluctuation p_{rms}' increases abruptly from around zero to a high value at a critical heater power ($K = 0.62$). The high-amplitude state is self-excited and periodic in time (see the insets of Fig. 1), indicating that the system has transitioned from a fixed point to a limit cycle via a Hopf bifurcation, with $K = 0.62$ being the Hopf point. Along the backward path (decreasing K), the system does not immediately revert to its initial fixed-point state, but instead remains on the limit-cycle branch until the heater power drops below the saddle-node point ($K = 0.52$). These Hopf and saddle-node points match those reported by Thomas *et al.* [44], demonstrating the accuracy of our
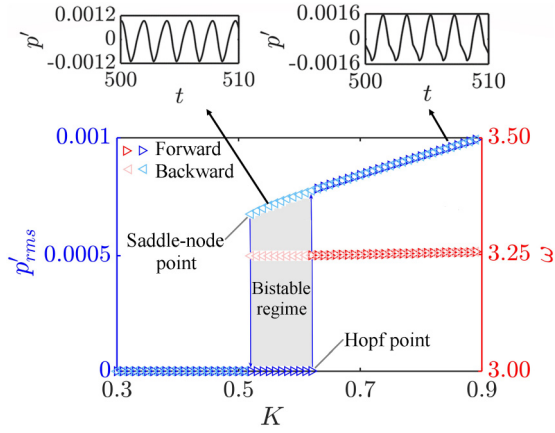
FIG. 1. Pressure amplitude (p'_{rms}) and limit-cycle frequency (ω) as functions of the heater power (K). The presence of a hysteretic bistable regime (gray shading) between the Hopf point ($K = 0.62$) and the saddle-node point ($K = 0.52$) indicates that the Hopf bifurcation is subcritical

numerical solution. The difference between the forward and backward paths leads to a hysteretic bistable regime (gray shading in Fig. 1), which indicates that the Hopf bifurcation is subcritical. In the limit-cycle regime, the system oscillates self-excitedly at a natural frequency of around $\omega = 2\pi f \approx 3.25$. As K increases, this limit-cycle frequency changes only slightly, but the limit-cycle amplitude increases markedly, with the pressure wave form becoming less sinusoidal owing to the emergence of harmonics (see the insets of Fig. 1).

Next we couple two Rijke tube oscillators together, using superscripts A and B to refer to tubes A and B, respectively. For tube A, the modified system of ODEs from Eqs. (10) and (11) becomes [44]

$$\frac{d\eta_j^A}{dt} = \dot{\eta}_j^A, \tag{14}$$

$$\frac{d\dot{\eta}_j^A}{dt} + 2\zeta_j\omega_j\dot{\eta}_j^A + \omega_j^2\eta_j^A$$
$$= -j\pi K^A\left[\sqrt{\left|\frac{1}{3} + u_h'^A(t - \tau_h)\right|} - \sqrt{\frac{1}{3}}\right]\sin(j\pi x_h)$$
$$+ \underbrace{\kappa_\tau\left[\dot{\eta}_j^B(t - \tau) - \dot{\eta}_j^A(t)\right]}_{\text{Time-delay coupling}} + \underbrace{\kappa_d\left(\dot{\eta}_j^B - \dot{\eta}_j^A\right)}_{\text{Dissipative coupling}}, \tag{15}$$

where switching the superscripts A and B gives the governing equations for tube B. Both the time-delay and dissipative coupling terms—whose strengths are denoted by κ_τ and κ_d, respectively—act on the acoustic pressure modes ($\dot{\eta}_j$), implying that their effect is not localized to a particular duct position [44]. The coupling delay time τ is a measure of the time required for information to propagate from one tube to the other. Both tubes have identical values of κ_τ, κ_d, and τ, so the time-delay and dissipative coupling terms are symmetric.

To investigate the effect of nonidentical oscillators, we adjust the heater powers of the two tubes (K^A and K^B) independently in a parameter space defined by $\alpha \equiv K^A + K^B = \{2, 3, 4\}$ and $\beta \equiv K^B/K^A = \{1, 1.5, 2.2, 3\}$. Thus, α quantifies the total power in the two tubes, while β quantifies the

mismatch in their heater powers. To introduce detuning, we fix ω^A at 3.25, but vary ω^B such that $0.75 \leqslant \omega^B/\omega^A \leqslant 1.34$. To quantify the changes in the steady-state amplitude due to coupling, we use the normalized oscillator amplitude, defined as the ratio of the root-mean-square pressure fluctuation with coupling to the same quantity without coupling, $\epsilon^A \equiv \langle p_{rms}'^A \rangle / p_{rms}'^A$ and $\epsilon^B \equiv \langle p_{rms}'^B \rangle / p_{rms}'^B$, where the angle brackets $\langle \rangle$ denote the presence of coupling.

III. RESULTS AND DISCUSSION

We consider three coupling schemes, in order of increasing complexity: dissipative coupling only (Sec. III A), time-delay coupling only (Sec. III B), and simultaneous time-delay and dissipative coupling (Sec. III C).

A. Dissipative coupling only

First we examine how α and β affect ϵ^A and ϵ^B when the two tubes interact via dissipative coupling only ($\kappa_d > 0$, $\kappa_\tau = 0$). Figure 2 shows ϵ^A and ϵ^B in a parameter space defined by κ_d and ω^B/ω^A. Before discussing the results, we note that when uncoupled, tube A at $\alpha = 2$ and $\beta = 3$ is at a fixed point (Fig. 1: $K^A = 0.5$) rather than a limit cycle, implying that ϵ^A is undefined; this specific case is therefore omitted from all the figures. In Fig. 2, four distinct types of amplitude responses can be identified: amplitude death, ϵ^A or $\epsilon^B \leqslant 0.01$ (cyan); amplitude reduction, $0.01 < \epsilon^A$ or $\epsilon^B < 1$ (blue); neutral response, ϵ^A or $\epsilon^B = 1$ (white); and amplitude amplification, ϵ^A or $\epsilon^B > 1$ (red).

For $\beta = 1$ (Fig. 2, identical oscillators), both tubes exhibit amplitude-death regions on either side of $\omega^B/\omega^A = 1$. Increasing β from 1 causes these regions to shrink, with this effect being more pronounced for $\omega^B/\omega^A > 1$ than for $\omega^B/\omega^A < 1$. Figure 3 shows time traces of the pressure fluctuation for a sample case where amplitude death occurs in both tubes as a result of dissipative coupling. Before the coupling is applied ($t < 200$), both tubes exhibit period-1 self-excited pressure oscillations of different limit-cycle amplitudes ($\beta = 1.5$). However, after the coupling is applied at $t = 200$, the oscillations in both tubes rapidly quench to a negligible amplitude, which is evidence of amplitude death. After the coupling is removed at $t = 400$, tube B takes a relatively long time to return to its initial period-1 state, while tube A remains quenched, indicating hysteresis. In summary, we find that introducing a mismatch in the initial limit-cycle oscillations, by introducing a mismatch in the heater powers, can hinder the emergence of amplitude death. Indeed, when both the heater power ratio and the total heater power are high ($\beta = 3$, $\alpha = 4$), neither tube exhibits amplitude death for the present test conditions.

Intriguingly, Fig. 2 also shows that when $\beta > 1$, amplitude amplification occurs, but only in the weaker oscillator (tube A). When β increases for a fixed α, the magnitude of amplitude amplification in tube A grows, without much affecting the magnitude of amplitude reduction in tube B, apart from a shrinkage in the regions of amplitude death. The shape of the amplitude-amplification region resembles that of the classic 1:1 Arnold tongue found in unidirectionally coupled systems undergoing forced synchronization [3]. Here the strength of
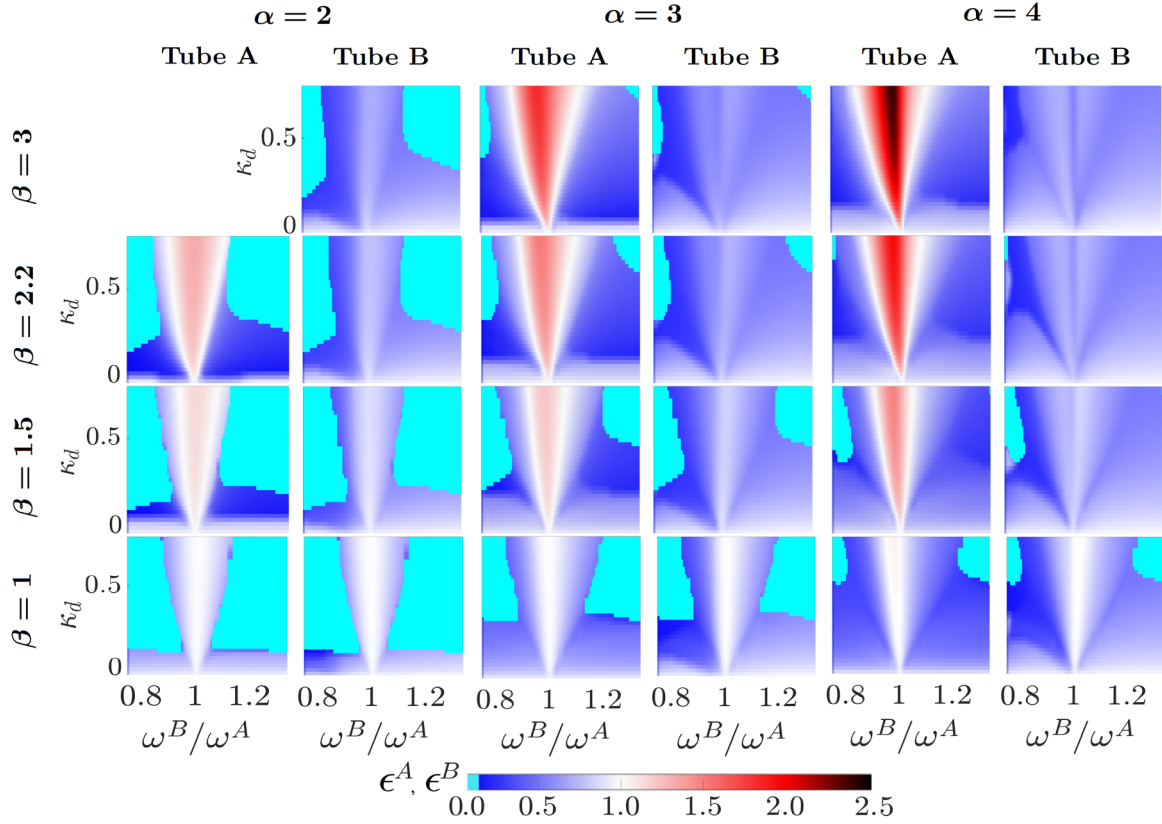
FIG. 2. Dissipative coupling only ($\kappa_\tau = 0$): the normalized oscillator amplitude ($\epsilon^A \equiv \langle p'^A_{rms}\rangle/p'^A_{rms}$, $\epsilon^B \equiv \langle p'^B_{rms}\rangle/p'^B_{rms}$) shown in a parameter space defined by the dissipative coupling strength (κ_d) and the frequency ratio (ω^B/ω^A). Focus is placed on the effect of the heater power ratio ($\beta \equiv K^B/K^A$) and the total heater power ($\alpha \equiv K^A + K^B$).

the dissipative coupling (κ_d) acts as an effective forcing amplitude, causing the region of amplitude amplification to widen on both sides of $\omega^B/\omega^A = 1$. When α increases for a fixed $\beta > 1$, the magnitude of amplitude amplification grows in tube A, while the regions of amplitude death shrink in both tubes, vanishing entirely at $\alpha = 4$ and $\beta = 3$ for the present range of frequency ratios.

Our report of amplitude amplification in a system of coupled thermoacoustic oscillators is important because practical combustion devices sometimes operate with spatially nonuniform thermal loads or damping. Knowing the system and
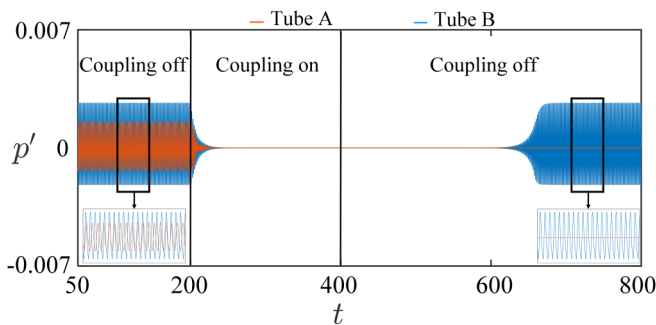

FIG. 3. Time traces of the pressure fluctuation for a sample case where amplitude death occurs in both tubes as a result of dissipative coupling only. The system and coupling parameters are $\alpha = 2$, $\beta = 1.5$, $\kappa_d = 0.5$, $\kappa_\tau = 0$, and $\omega^B/\omega^A = 1.2$.
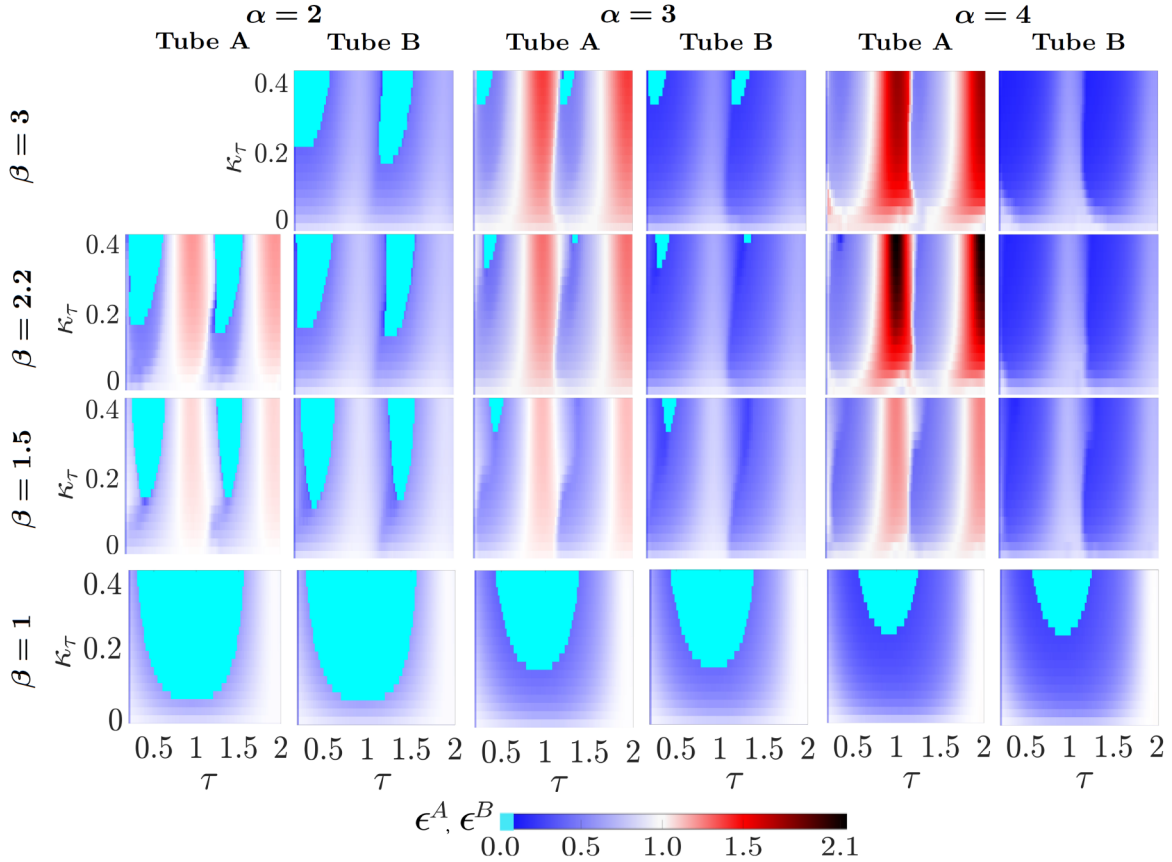
coupling parameters at which such oscillator mismatches can promote thermoacoustic instability would help to avoid potentially dangerous operating conditions.

B. Time-delay coupling only

Next we examine how α and β affect ϵ^A and ϵ^B when the two tubes interact via time-delay coupling only ($\kappa_d = 0$, $\kappa_\tau > 0$) with $\omega^A = \omega^B$. Figure 4 shows ϵ^A and ϵ^B in a parameter space defined by κ_τ and τ.

For $\beta = 1$ (Fig. 4, identical oscillators), both tubes exhibit a central region of amplitude death, with no evidence of amplitude amplification. As α increases, the amplitude-death region shrinks, but remains centered at $\tau \approx T/2 \approx 1$ (T is the oscillation period), which is consistent with the numerical simulations of Thomas *et al.* [44] and the laboratory experiments of Hyodo *et al.* [36].

For $\beta > 1$ (Fig. 4, nonidentical oscillators), the central region of amplitude death seen in both tubes at $\beta = 1$ splits into separate islands at $\tau \approx T/4 \approx 0.5$ and $\tau \approx 3T/4 \approx 1.5$. As α increases, these islands remain centered at the same values of τ, but shrink until disappearing altogether at $\alpha = 4$. As is the case with dissipative coupling (Sec. III A), we find that amplitude amplification occurs only in the presence of a power mismatch ($\beta > 1$) and only in the weaker oscillator (tube A). Increasing β or α is found to increase the magnitude of amplitude amplification without much affecting the coupling delay times at which it occurs, $\tau \approx T/2 \approx 1$

FIG. 4. Time-delay coupling only ($\kappa_d = 0$): the normalized oscillator amplitude ($\epsilon^A \equiv \langle p'^A_{rms} \rangle / p'^A_{rms}, \epsilon^B \equiv \langle p'^B_{rms} \rangle / p'^B_{rms}$) shown in a parameter space defined by the time-delay coupling strength (κ_τ) and the coupling delay time (τ) with $\omega^A = \omega^B$. The period of the fundamental oscillation is $T = 1.93$. Focus is placed on the effect of the heater power ratio ($\beta \equiv K^B/K^A$) and the total heater power ($\alpha \equiv K^A + K^B$).

and $\tau \approx T \approx 2$. Figure 5 shows time traces of the pressure fluctuation for a sample case where amplitude amplification occurs in tube A, while amplitude reduction occurs in tube B. Before the application of time-delay coupling ($t < 200$), both tubes exhibit self-excited pressure oscillations of different limit-cycle amplitudes ($\beta = 2.2$). Compared with the case of Fig. 3, here the values of K^A and K^B are higher, which causes the pressure wave forms in both tubes to undergo
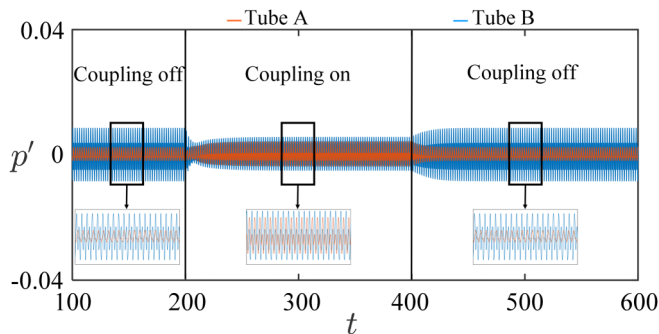

FIG. 5. Time traces of the pressure fluctuation for a sample case where amplitude amplification occurs in tube A, while amplitude reduction occurs in tube B, both as a result of time-delay coupling. The system and coupling parameters are $\alpha = 4$, $\beta = 2.2$, $\kappa_d = 0$, $\kappa_\tau = 0.3$, $\omega^A = \omega^B$, and $\tau = 1$.

period doubling. This results in period-2 oscillations, similar to those observed numerically by Thomas *et al.* [44] and experimentally by Gopalakrishnan and Sujith [55] at high heater powers. Following the application of coupling at $t = 200$, the oscillations in tube A become amplified, while those in tube B become attenuated. After the removal of coupling at $t = 400$, both tubes return to their initial limit-cycle states, with no sign of hysteresis.

Crucially, we note that a coupling delay time ($\tau \approx 1$) that induces amplitude death in identical oscillators ($\beta = 1$) could induce amplitude amplification in nonidentical oscillators ($\beta > 1$). Thus, if time-delay coupling is used alone to quench thermoacoustic oscillations via amplitude death, then it is essential to account for oscillator differences. Otherwise, a state of amplitude death could turn into a state of amplitude amplification if a mismatch in the heater powers were to emerge, either via unintentional processes or by design.

C. Simultaneous time-delay and dissipative coupling

We now examine the effect of applying both time-delay and dissipative coupling simultaneously. Figure 6 shows ϵ^A and ϵ^B in a three-dimensional parameter space defined by κ_d, κ_τ, and τ. The detuning is nonzero, with frequency ratio $\omega^B/\omega^A = 0.95$. To aid visualization, we show two-dimensional slices at $\kappa_d = 0$, 0.3, and 0.6.
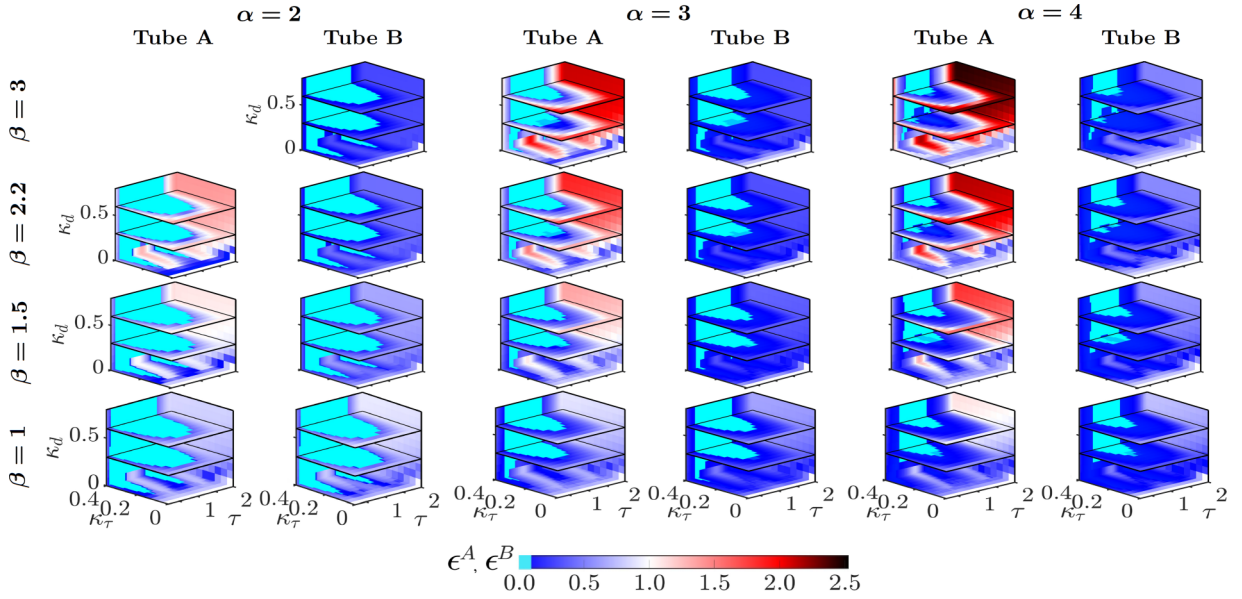
FIG. 6. Simultaneous time-delay and dissipative coupling: the normalized oscillator amplitude ($\epsilon^A \equiv \langle p'^A_{rms}\rangle / p'^A_{rms}$, $\epsilon^B \equiv \langle p'^B_{rms}\rangle / p'^B_{rms}$) shown in a three-dimensional parameter space defined by the dissipative coupling strength (κ_d), the time-delay coupling strength (κ_τ), and the coupling delay time (τ). The frequency ratio is $\omega^B/\omega^A = 0.95$. Focus is placed on the effect of the heater power ratio ($\beta \equiv K^B/K^A$) and the total heater power ($\alpha \equiv K^A + K^B$)

As is the case with dissipative (Sec. III A) and time-delay (Sec. III B) coupling, we find that in most cases, only in the weaker oscillator (tube A) under nonidentical power conditions ($\beta > 1$) can amplitude amplification occur. Increasing κ_τ for a fixed κ_d is found to shrink the regions of amplitude amplification, while enlarging the regions of amplitude death. Increasing α or β is found to increase the magnitude of amplitude amplification in the weaker oscillator (tube A), while shrinking the regions of amplitude death in both oscillators. Amplitude amplification tends to occur when κ_d is large and when either τ is large or κ_τ is small. By contrast, amplitude death tends to occur when κ_τ is large.

Comparing Figs. 4 and 6, we find that introducing finite detuning in a purely time-delay coupled system at $\beta = 1$ (see Fig. 6, bottom two-dimensional slice at $\kappa_d = 0$) has an effect similar to that of introducing a power mismatch ($\beta > 1$): a central region of amplitude death at $\tau \approx T/2 \approx 1$ (Fig. 4) splits into multiple branches (Fig. 6), but these eventually merge back when dissipative coupling is applied as well ($\kappa_d > 0$).

Figure 7 is analogous to Fig. 6, but for a lower frequency ratio, $\omega^B/\omega^A = 0.90$. Comparing the two figures, we find no significant changes in the amplitude-death regions, but marked reductions in the magnitude
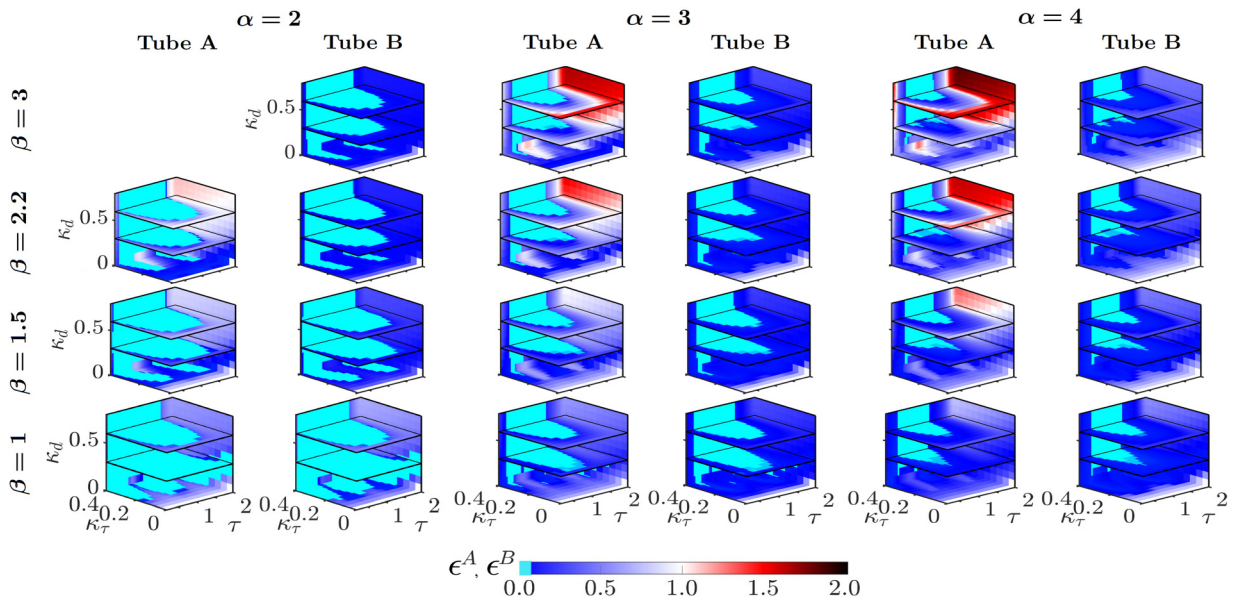

FIG. 7. The same as for Fig. 6, but at a lower frequency ratio, $\omega^B/\omega^A = 0.90$.

and size of the amplitude-amplification regions. Taken together, these observations show that when both time-delay and dissipative coupling are applied simultaneously, even small mismatches in the initial limit-cycle frequencies or amplitudes can lead to large changes in amplitude amplification.

IV. CONCLUSIONS

In this numerical study, we have investigated the effect of nonidentical heater powers on the quenching and amplification of two self-excited thermoacoustic oscillators, each modeled as a prototypical Rijke tube. We coupled the two oscillators together via dissipative coupling only, then via time-delay coupling only, and finally via both dissipative and time-delay coupling. By parametrizing the system in terms of the heater power ratio (β) and the total heater power (α), we were able to identify several key findings.

When only dissipative coupling is applied, introducing nonidentical heater powers ($\beta > 1$) is found to produce a central region of amplitude amplification in the weaker oscillator (tube A), resembling the shape of the classic 1:1 Arnold tongue found in unidirectionally coupled systems undergoing forced synchronization. As β or α increases, the magnitude of amplitude amplification grows in the weaker oscillator (tube A), while the regions of amplitude death shrink in both oscillators.

When only time-delay coupling is applied, increasing β or α is found to shrink the amplitude-death regions in both oscillators. Switching from identical oscillators ($\beta = 1$) to nonidentical oscillators ($\beta > 1$) causes a central amplitude-death region to split into multiple islands at $\tau = T/4$ and $3T/4$. Meanwhile, amplitude-amplification regions emerge at $\tau = T/2$ and T and grow in magnitude as β increases. However, the range of τ over which amplitude amplification occurs remains largely constant as β and α are varied for nonidentical oscillators.

When both time-delay and dissipative coupling are applied simultaneously, increasing β or α is found to shrink the amplitude-death regions in both oscillators, while increasing the magnitude of amplitude amplification in the weaker oscillator (tube A). Detuning is found to have only a minor influence on the amplitude-death regions, but a major influence on both the size and magnitude of the amplitude-amplification regions.

Collectively, these findings show that the presence of nonidentical thermal loads in a coupled thermoacoustic system can have profound and unexpected effects on the overall amplitude response. In particular, we have shown that although increasing β can generally shrink the regions of amplitude death, it can also induce amplitude amplification, particularly at high α. In some coupled thermoacoustic systems optimized for nominally stable operation (e.g., can-annular gas turbines), the occurrence of amplitude amplification may lead to flow oscillations strong enough to accelerate cyclic fatigue and degrade system efficiency and reliability. Knowing the system and coupling parameters at which amplitude death and amplitude amplification occur can aid in the design of these and other coupled oscillator systems.

[1] P. C. Matthews and S. H. Strogatz, Phase Diagram for the Collective Behavior of Limit-Cycle Oscillators, Phys. Rev. Lett. **65**, 1701 (1990).

[2] Y. Kuramoto, Cooperative dynamics of oscillator community: A study based on lattice of rings, Prog. Theor. Phys. Suppl. **79**, 223 (1984).

[3] A. Pikovsky, M. Rosenblum, and J. Kurths, *Synchronization: A Universal Concept in Nonlinear Sciences* (Cambridge University Press, Cambridge, 2003).

[4] J. W. S. B. Rayleigh, *The Theory of Sound*, Vol. 2 (Macmillan, London, 1896).

[5] R. E. Mirollo and S. H. Strogatz, Amplitude death in an array of limit-cycle oscillators, J. Stat. Phys. **60**, 245 (1990).

[6] M. Abel, K. Ahnert, and S. Bergweiler, Synchronization of Sound Sources, Phys. Rev. Lett. **103**, 114301 (2009).

[7] G. Saxena, A. Prasad, and R. Ramaswamy, Amplitude death: The emergence of stationarity in coupled nonlinear systems, Phys. Rep. **521**, 205 (2012).

[8] D. V. Ramana Reddy, A. Sen, and G. L. Johnston, Experimental Evidence of Time-Delay-Induced Death in Coupled Limit-Cycle Oscillators, Phys. Rev. Lett. **85**, 3381 (2000).

[9] K. Zeyer, M. Mangold, and E. Gilles, Experimentally coupled thermokinetic oscillators: Phase death and rhythmogenesis, J. Phys. Chem. A **105**, 7216 (2001).

[10] A. Balanov, N. Janson, D. Postnov, and O. Sosnovtseva, *Synchronization: From Simple to Complex* (Springer Science & Business Media, Berlin, 2008).

[11] R. I. Sujith and S. A. Pawar, *Thermoacoustic instability: A complex systems perspective* (Springer Nature, London, 2021).

[12] T. C. Lieuwen and V. Yang, *Combustion Instabilities in Gas Turbine Engines: Operational Experience, fundamental Mechanisms, and Modeling* (American Institute of Aeronautics and Astronautics, 2005).

[13] S. J. Shanbhogue, S. Husain, and T. Lieuwen, Lean blowoff of bluff body stabilized flames: Scaling and dynamics, Prog. Energy Combust. Sci. **35**, 98 (2009).

[14] S. Candel, Combustion dynamics and control: Progress and challenges, Proc. Combust. Inst. **29**, 1 (2002).

[15] Y. Huang and V. Yang, Dynamics and stability of lean-premixed swirl-stabilized combustion, Prog. Energy Combust. Sci. **35**, 293 (2009).

[16] T. Poinsot, Prediction and control of combustion instabilities in real engines, Proc. Combust. Inst. **36**, 1 (2017).

[17] S. Murayama and H. Gotoda, Attenuation behavior of thermoacoustic combustion instability analyzed by a complex-network- and synchronization-based approach, Phys. Rev. E **99**, 052222 (2019).

[18] R. I. Sujith and V. R. Unni, Dynamical systems and complex systems theory to study unsteady combustion, P. Combust. Inst. **38**, 3445 (2021).

[19] R. I. Sujith and V. R. Unni, Complex system approach to investigate and mitigate thermoacoustic instability in turbulent combustors, Phys. Fluids **32**, 061401 (2020).

[20] A. P. Dowling and A. S. Morgans, Feedback control of combustion oscillations, Annu. Rev. Fluid Mech. **37**, 151 (2005).

[21] H. Gotoda, Y. Shinoda, M. Kobayashi, Y. Okuno, and S. Tachibana, Detection and control of combustion instability based on the concept of dynamical system theory, Phys. Rev. E **89**, 022910 (2014).

[22] D. Zhao and X. Li, A review of acoustic dampers applied to combustion chambers in aerospace industry, Prog. Aerosp. Sci. **74**, 114 (2015).

[23] D. Zhao, Z. Lu, H. Zhao, X. Li, B. Wang, and P. Liu, A review of active control approaches in stabilizing combustion systems in aerospace industry, Prog. Aerosp. Sci. **97**, 35 (2018).

[24] Y. Guan, M. Murugesan, and L. K. B. Li, Strange nonchaotic and chaotic attractors in a self-excited thermoacoustic oscillator subjected to external periodic forcing, Chaos **28**, 093109 (2018).

[25] Y. Guan, V. Gupta, M. Wan, and L. K. B. Li, Forced synchronization of quasiperiodic oscillations in a thermoacoustic system, J. Fluid Mech. **879**, 390 (2019).

[26] Y. Guan, W. He, M. Murugesan, Q. Li, P. Liu, and L. K. B. Li, Control of self-excited thermoacoustic oscillations using transient forcing, hysteresis and mode switching, Combust. Flame **202**, 262 (2019).

[27] T. Kobayashi, S. Murayama, T. Hachijo, and H. Gotoda, Early Detection of Thermoacoustic Combustion Instability Using a Methodology Combining Complex Networks and Machine Learning, Phys. Rev. Appl. **11**, 064034 (2019).

[28] Y. Guan, V. Gupta, K. Kashinath, and L. K. B. Li, Open-loop control of periodic thermoacoustic oscillations: Experiments and low-order modelling in a synchronization framework, Proc. Combust. Inst. **37**, 5315 (2019).

[29] P. Kaufmann, W. Krebs, R. Valdes, and U. Wever, 3D thermoacoustic properties of single can and multi can combustor configurations, in *Proceedings of the ASME Turbo Expo 2008: Power for Land, Sea, and Air*, Vol. 3, Combustion, Fuels and Emissions, Parts A and B. Berlin, Germany (2008), pp. 527–538.

[30] S. Luque, V. Kanjirakkad, I. Aslanidou, R. Lubbock, B. Rosic, and S. Uchida, A new experimental facility to investigate combustor–turbine interactions in gas turbines with multiple can combustors, J. Eng. Gas Turb. Power **137**, 051503 (2015).

[31] F. Farisco, L. Panek, and J. B. W. Kok, Thermo-acoustic cross-talk between cans in a can-annular combustor, Intl. J. Spray Combust. **9**, 452 (2017).

[32] G. Bonciolini and N. Noiray, Synchronization of thermoacoustic modes in sequential combustors, J. Eng. Gas Turb. Power **141**, 031010 (2019).

[33] G. Ghirardo, C. Di Giovine, J. P. Moeck, and M. R. Bothien, Thermoacoustics of can-annular combustors, J. Eng. Gas Turb. Power **141**, 011007 (2019).

[34] Y. Guan, K. Moon, K. T. Kim, and L. K. B. Li, Synchronization and chimeras in a network of four ring-coupled thermoacoustic oscillators, J. Fluid Mech. **938**, A5 (2022).

[35] Y. Guan, K. Moon, K. T. Kim, and L. K. B. Li, Low-order modeling of the mutual synchronization between two turbulent thermoacoustic oscillators, Phys. Rev. E **104**, 024216 (2021).

[36] H. Hyodo, M. Iwasaki, and T. Biwa, Suppression of Rijke tube oscillations by delay coupling, J. Appl. Phys. **128**, 094902 (2020).

[37] S. Dange, K. Manoj, S. Banerjee, S. A. Pawar, S. Mondal, and R. I. Sujith, Oscillation quenching and phase-flip bifurcation in coupled thermoacoustic systems, Chaos **29**, 093135 (2019).

[38] T. Biwa, S. Tozuka, and T. Yazaki, Amplitude Death in Coupled Thermoacoustic Oscillators, Phys. Rev. Appl. **3**, 034006 (2015).

[39] H. Hyodo and T. Biwa, Stabilization of thermoacoustic oscillators by delay coupling, Phys. Rev. E **98**, 052223 (2018).

[40] H. Jegal, K. Moon, J. Gu, L. K. B. Li, and K. T. Kim, Mutual synchronization of two lean-premixed gas turbine combustors: Phase locking and amplitude death, Combust. Flame **206**, 424 (2019).

[41] K. Moon, Y. Guan, L. K. B. Li, and K. T. Kim, Mutual synchronization of two flame-driven thermoacoustic oscillators: Dissipative and time-delayed coupling effects, Chaos **30**, 023110 (2020).

[42] A. Prasad, J. Kurths, S. K. Dana, and R. Ramaswamy, Phase-flip bifurcation induced by time delay, Phys. Rev. E **74**, 035204(R) (2006).

[43] D. G. Aronson, G. B. Ermentrout, and N. Kopell, Amplitude response of coupled oscillators, Physica D **41**, 403 (1990).

[44] N. Thomas, S. Mondal, S. A. Pawar, and R. I. Sujith, Effect of time-delay and dissipative coupling on amplitude death in coupled thermoacoustic oscillators, Chaos **28**, 033119 (2018).

[45] D. V. Ramana Reddy, A. Sen, and G. L. Johnston, Time Delay Induced Death in Coupled Limit Cycle Oscillators, Phys. Rev. Lett. **80**, 5109 (1998).

[46] S. Mondal, A. Mukhopadhyay, and S. Sen, Effects of inlet conditions on dynamics of a thermal pulse combustor, Combust. Theory Model. **16**, 59 (2012).

[47] M.-D. Wei and J.-C. Lun, Amplitude death in coupled chaotic solid-state lasers with cavity-configuration-dependent instabilities, Appl. Phys. Lett. **91**, 061121 (2007).

[48] K. Balasubramanian and R. Sujith, Thermoacoustic instability in a Rijke tube: Non-normality and nonlinearity, Phys. Fluids **20**, 044103 (2008).

[49] M. P. Juniper and R. I. Sujith, Sensitivity and nonlinearity of thermoacoustic oscillations, Annu. Rev. Fluid Mech. **50**, 661 (2018).

[50] P. Subramanian, S. Mariappan, R. Sujith, and P. Wahi, Bifurcation analysis of thermoacoustic instability in a horizontal Rijke tube, Intl. J. Spray Combust. Dyn. **2**, 325 (2010).

[51] L. V. King, On the convection of heat from small cylinders in a stream of fluid: Determination of the convection constants of small platinum wires with applications to hot-wire anemometry, Philos. Trans. R. Soc. London, Ser. A **214**, 373 (1914).

[52] M. A. Heckl, Non-linear acoustic effects in the Rijke tube, Acta Acust. United Ac. **72**, 63 (1990).

[53] J. D. Sterling and E. E. Zukoski, Nonlinear dynamics of laboratory combustor pressure oscillations, Combust. Sci. Technol. **77**, 225 (1991).

[54] K. I. Matveev and F. E. C. Culick, A model for combustion instability involving vortex shedding, Combust. Sci. Technol. **175**, 1059 (2003).

[55] E. A. Gopalakrishnan and R. I. Sujith, Influence of system parameters on the hysteresis characteristics of a horizontal Rijke tube, Intl. J. Spray Combust. Dyn. **6**, 293 (2014).